Chemical Science

ROYAL SOCIETY OF CHEMISTRY

EDGE ARTICLE

View Article Online
View Journal | View Issue

Cite this: *Chem. Sci.*, 2024, **15**, 2047

All publication charges for this article have been paid for by the Royal Society of Chemistry

Mono- and bis-Pd(II) complexes of N-confused dithiahexaphyrin(1.1.1.1.1.0) with the absorption and aromaticity modulated by Pd(II) coordination, macrocycle contraction and ancillary ligands†

Meng Sun,[a] Yongshu Xie, *[ab] Glib Baryshnikov,[c] Chengjie Li,[a] Feng Sha,[a] Xinyan Wu,[a] Hans Ågren,[d] Shijun Li[b] and Qizhao Li *[a]

Received 16th October 2023
Accepted 2nd January 2024

DOI: 10.1039/d3sc05473j

rsc.li/chemical-science

To further enrich the coordination chemistry of hexaphyrins and probe the underlying property–structural correlations, N-confused dithiahexaphyrin(1.1.1.1.1.0) (**1**) with 26 π-electron Hückel aromaticity was synthesized. Based on its unprecedented two unsymmetrical cavities, five palladium complexes **2**, **3**, **4-Ph**, **4-Cl** and **5** have been successfully synthesized under various coordinations. Thus, two mono-Pd(II) complexes **2** and **3** with the Pd(II) atom coordinated in the two different cavities were obtained by treating **1** with palladium reagents $PdCl_2$, and $(PPh_3)_2PdCl_2$ respectively. On this basis, bis-Pd(II) complexes **4-Ph** and **4-Cl** were synthesized by treating **2** and **3** with $(PPh_3)_2PdCl_2$ and $PdCl_2$, respectively. As a result, both **4-Ph** and **4-Cl** contain two Pd(II) atoms coordinated within the two cavities, with one of the Pd(II) atoms further coordinated to a triphenylphosphine ligand in addition to an anionic ancillary ligand of Ph^- and Cl^-, respectively. Notably, a further contracted mono-Pd(II) complex **5** was synthesized by treating **1** with $Pd(PPh_3)_4$ by eliminating one of the *meso*-carbon atoms together with the corresponding C_6F_5 moiety. These complexes present tunable 26 π aromaticity and NIR absorption up to 1060 nm. This work provides an effective approach for developing distinctive porphyrinoid Pd(II) complexes from a single porphyrinoid, without resorting to tedious syntheses of a series of porphyrinoid ligands.

Introduction

As a class of tetrapyrrole macrocyclic compounds, porphyrins and their metal complexes, namely, metalloporphyrins exist widely in nature and play important roles in materials science and life activities, owing to their rich photophysical, electronic and catalytic properties.[1–6] In recent years, the tetrapyrrolic frameworks of porphyrins have been modified to afford various porphyrin analogues termed as porphyrinoids.[7–21] Thus, N-confused porphyrins,[10,11] core-modified porphyrins[22–27] and expanded porphyrins[28–30] have been developed by incorporating an α,β′-linked pyrrole, using heteroatoms like O, S and Se in place of the N atoms, and employing more than four pyrrolic units, respectively (Fig. 1a–c). As a result, these porphyrinoids exhibit much richer coordination behavior. For example, hexaphyrins may coordinate to either one or two metal ions within the two cavities, and the coordinated metal ions exhibit rich oxidation states.[31–48] In addition, the N-confused pyrrole unit may trigger interesting macrocycle transformations and thus further modulate the coordination behavior.[49–55] These metal complexes are promising for applications in various areas like catalytic, photoelectric and biomedical materials.[56–67]

To further enrich the coordination chemistry of hexaphyrins and probe the underlying property–structural correlations for porphyrinoid complexes, herein we report N-confused dithiahexaphyrin **1**, which has been synthesized by simultaneously incorporating an N-confused pyrrole unit and a bithiophene unit into a hexaphyrin framework (Fig. 1d). As a result, **1** possesses two coordination cavities with different sizes and coordinating atoms employable for metal coordination. Considering that rich structural diversity has been reported for Pd(II) complexes of porphyrinoids involving Pd(II)–C and Pd(II)–N coordination bonds,[50,51] and the presence of the Pd(II)–C

[a]*Key Laboratory for Advanced Materials, Frontiers Science Center for Materiobiology and Dynamic Chemistry, Institute of Fine Chemicals, School of Chemistry and Molecular Engineering, East China University of Science and Technology, Shanghai 200237, China. E-mail: yshxie@ecust.edu.cn; zhaolq@ecust.edu.cn*

[b]*College of Material, Chemistry and Chemical Engineering, Key Laboratory of Organosilicon Chemistry and Material Technology of Ministry of Education, Hangzhou Normal University, Hangzhou, 311121, China*

[c]*Department of Science and Technology, Laboratory of Organic Electronics, Linköping University, SE-601 74 Norrköping, Sweden*

[d]*Department of Physics and Astronomy, Uppsala University, SE-751 20 Uppsala, Sweden*

† Electronic supplementary information (ESI) available. CCDC 2277039–2277043. For ESI and crystallographic data in CIF or other electronic format see DOI: https://doi.org/10.1039/d3sc05473j

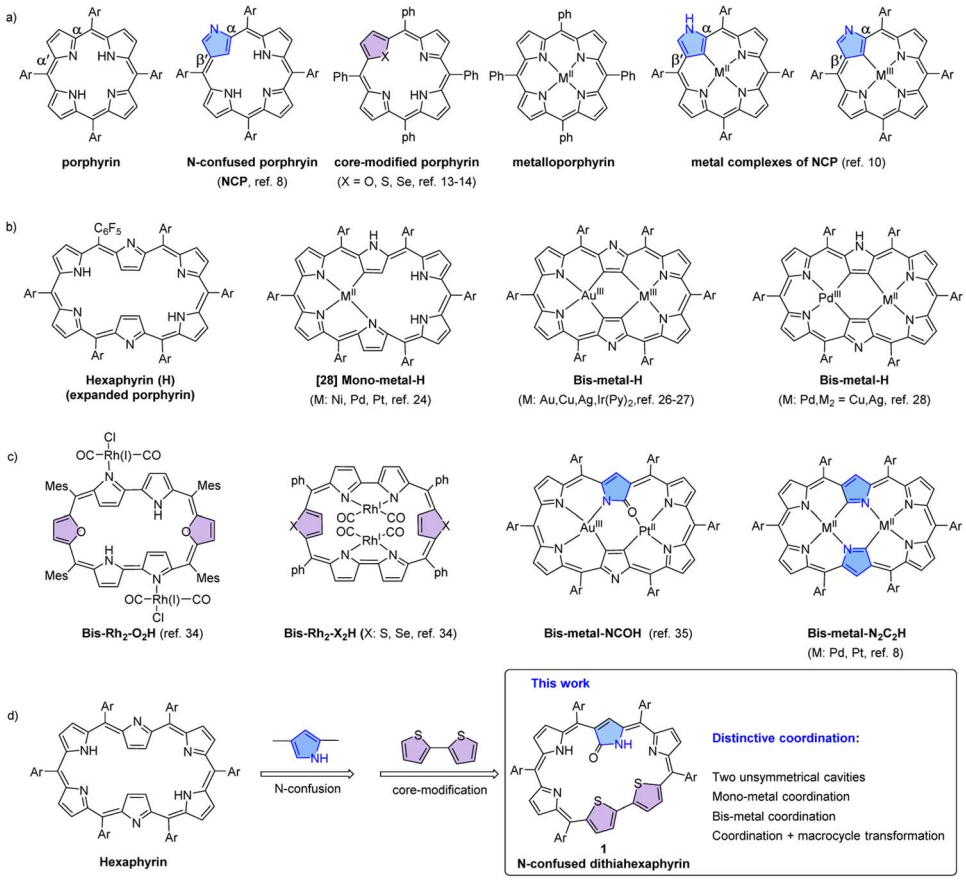

Fig. 1 Chemical structures of free bases and metal complexes of porphyrin and its tetrapyrrolic analogues (a), hexaphyrin (b) and its analogues (c), and N-confused dithiahexaphyrin (d).

bonds may facilitate cross-coupling reactions and macrocycle interconversions,[68–70] **1** was treated with various palladium reagents to afford a series of Pd(II) complexes. Interestingly, five mono-Pd(II) and bis-Pd(II) complexes **2**, **3**, **4-Ph**, **4-Cl** and **5** have been synthesized. Thus, successive coordination of **1** with $PdCl_2$ and $(PPh_3)_2PdCl_2$ in CH_2Cl_2 and MeOH afforded **2** and **4-Ph**, respectively. Interestingly, when the reaction sequence was reversed, complexes **3** and **4-Cl** were obtained, respectively. As a result, the Pd(II) atom in the mono-Pd(II) complexes **2** and **3** is coordinated in the two different cavities, respectively. On the other hand, different ancillary anionic ligands Ph^- and Cl^- are observed for bis-Pd(II) complexes **4-Ph** and **4-Cl**, respectively. Notably, the treatment of **1** with $Pd(PPh_3)_4$ in CH_2Cl_2 afforded a third mono-Pd(II) complex **5**, with the macrocycle further contracted by eliminating one of the *meso*-carbon atoms and the corresponding C_6F_5 moiety. These results provide examples for synthesizing unprecedented palladium complexes with tunable structures and properties from a single porphyrinoid ligand with the advantages of avoiding tedious syntheses of a series of porphyrinoid ligands.

Results and discussion

Initially, N-confused dithiahexaphyrin(1.1.1.1.1.0) (**1**) was conveniently synthesized as a violet solid in the yield of 12% by condensing N-confused bilane with bithiophene diol in the presence of $BF_3 \cdot Et_2O$, followed by oxidation with DDQ (see ESI†). The high-resolution mass spectrometry (HRMS) of **1** shows a pseudo molecular ion peak at $m/z = 1332.0127$ ($[M]^+$, calcd for $C_{59}H_{13}F_{25}N_4OS_2$: 1332.0126) (Fig. S2†), indicative of a dithiahexaphyrin(1.1.1.1.1.0) structure with the attachment of an oxygen atom (Scheme 1). With **1** in hand, it was coordinated with Pd(II) under various conditions. When **1** was coordinated with the respective Pd(II) reagents of $PdCl_2$ and $(PPh_3)_2PdCl_2$ in a mixed solvent of CH_2Cl_2/MeOH, mono-Pd complexes **2** and **3** were obtained as blue and dark blue solids in the yields of 45% and 24%, respectively (Scheme 1). The HRMS of **2** and **3** reveals pseudo molecular ion peaks at $m/z = 1435.9018$ ($[M]^+$, calcd for $C_{59}H_{11}F_{25}N_4OPdS_2$: 1435.9023) (Fig. S3†) and $m/z = 1733.9787$ ($[M]^+$, calcd for $C_{77}H_{27}ClF_{25}N_4OPPdS_2$: 1733.9784) (Fig. S4†), respectively, indicative of mono-Pd(II) coordination structures of **2** and **3** and additional ancillary coordination in **3** (*vide infra*). On this basis, it may be anticipated that the mono-Pd(II) complexes can be further coordinated with alternative Pd(II) reagents to afford the corresponding bis-Pd(II) complexes. Thus, **2** and **3** were further coordinated with $(PPh_3)_2PdCl_2$ and $PdCl_2$, respectively. As a result, bis-Pd(II) complexes **4-Ph** and **4-Cl** were obtained as green solids in the yields of 31% and 37%, respectively. Although **4-Ph** can also be obtained by treating **2**

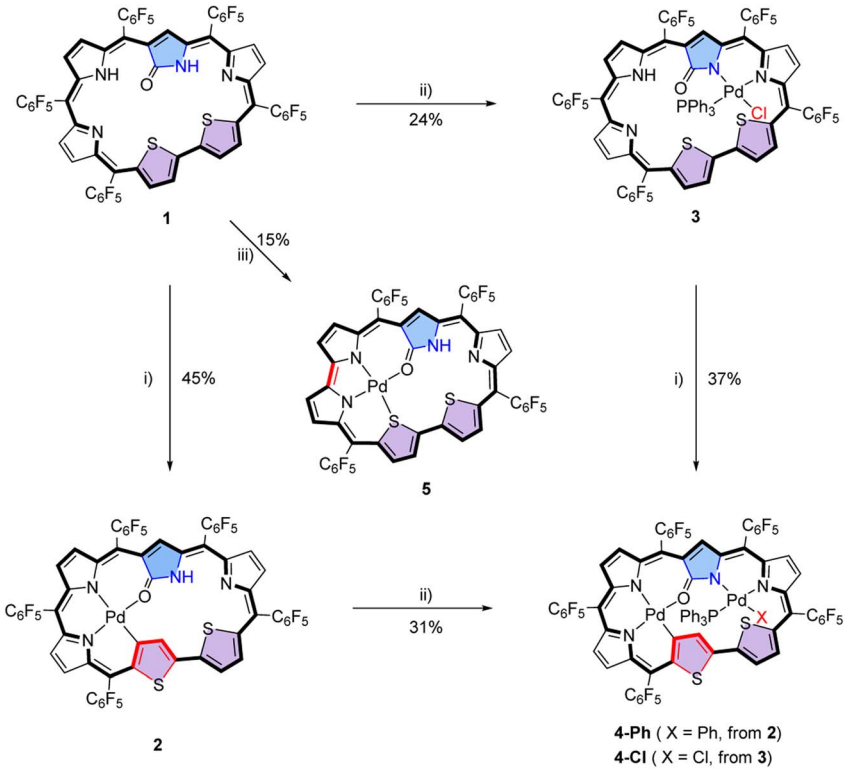

Scheme 1 Syntheses of complexes **2**, **3**, **4-Ph**/**4-Cl** and **5**, conditions: (i) $PdCl_2$ in CH_2Cl_2/MeOH with NaOAc; (ii) $(PPh_3)_2PdCl_2$ in CH_2Cl_2/MeOH with NaOAc; and (iii) $Pd(PPh_3)_4$ in CH_2Cl_2.

with $Pd(PPh_3)_4$, and **4-Cl** can also be obtained by treating **3** with other palladium salts like $Pd(PPh_3)_4$, $(PPh_3)_2PdCl_2$ and $Pd(OAc)_2$, the yields are all very low. The HRMS of bis-Pd complex **4-Ph** reveals a molecular ion peak at $m/z = 1879.9299$ ($[M]^+$, calcd for $C_{83}H_{30}F_{25}N_4OPPd_2S_2$: 1879.9297) (Fig. S5†), consistent with a bis-Pd complex structure containing ancillary PPh_3 and phenyl ligands. Whereas, the pseudo molecular ion peak observed for **4-Cl** at $m/z = 1887.8573$ ($[M]^+$, calcd for $C_{77}H_{25}ClF_{25}N_4OPPd_2S_2$: 1887.8588) reveals a bis-Pd structure with ancillary PPh_3 and chloro ligands (Fig. S6†). The only structural difference between **4-Ph** and **4-Cl** lies in their ancillary ligands, but they could not be transformed into each other even after repeated trials, indicative of strong coordination of the ancillary anionic ligand, which is thus difficult to substitute. Inspired by the syntheses of mono-Pd(II) complexes **2** and **3** by employing different Pd(II) reagents, **1** was further coordinated with additional Pd(II) reagents. Interestingly, when $Pd(PPh_3)_4$ was used to coordinate with **1** in CH_2Cl_2, another mono-Pd(II) complex **5** were obtained as purple solid in the yield of 15%. The HRMS of **5** reveals a pseudo molecular ion peak at $m/z = 1257.9174$ ($[M]^+$, calcd for $C_{52}H_{12}F_{20}N_4OPdS_2$: 1257.9179) (Fig. S7†), which reveals the elimination of a C_7F_5 moiety, compared with **2**. These data indicate that the hexaphyrin ligand has been further contracted by eliminating one of the *meso*-carbon atoms as well as the corresponding C_6F_5 moiety on the basis of the mono-Pd(II) complex **2**. Based on these results, a plausible reaction mechanism has been proposed for the generation of **5** (Fig. S8†), which involves the coordination of a Pd(0) atom within the cavity together with a PPh_3 ligand. Similar to the synthesis of **5** from the reaction of $Pd(PPh_3)_4$ with **1** in CH_2Cl_2, **5** was also detected when PPh_3 was added to the solution of **1** and $Pd(OAc)_2$ in CH_2Cl_2. In contrast, **5** could not detected when PPh_3 was replaced by more bulky phosphine ligands like BINAP, Sphos, $(tBu)_3PHBF_4$, and DPEphos. These results indicate that the coordination of the Pd(0) atom together with the bulky ligand may be hampered by serious steric hindrance induced by the bulky ligand. Considering that complex **3** still possesses a noncoordinated cavity similar to that of free base **1**, it could be anticipated that **3** may undergo a reaction similar to that of **1** to afford a contracted product similar to **5**. Thus, complex **3** was treated with $Pd(PPh_3)_4$, but no contracted product could be obtained, which may be related to the difficulty in Pd(0) coordination because the cavity cannot be easily adapted to satisfy the coordination requirement of Pd(0) due to the more rigid structure of complex **3** than that of free base **1**. This inference is also evidenced by the very low yield of **4-Cl** obtained from the coordination of **3** with $Pd(PPh_3)_4$ (*vide supra*). Although complex **5** still possesses a noncoordinated cavity, no bis-Pd(II) complex could be obtained from **5**, which may be related to the insufficient size of the contracted structure.

Consistent with the HRMS data of **1** (*vide supra*), its ^1H NMR spectrum in $CDCl_3$ shows two NH signals in the relatively high field region ($\delta = 1.28$ and 1.50 ppm) and eleven CH protons in the relatively low field region ($\delta = 8.34$–10.70 ppm) (Fig. S11†), indicative of an aromatic macrocycle.[71] Consistently, single crystal X-ray diffraction analysis reveals that **1** possesses

a dithiahexaphyrin(1.1.1.1.1.0) macrocycle containing three normal pyrroles, an N-confused pyrrole and a bithiophene unit, with an oxygen atom attached to the α-position of the confused pyrrole C (Fig. 2a, b and S23†), which is also consistent with the HRMS data (*vide supra*). The C1–O1 bond length of 1.208 Å is typical for a C=O double bond. Within the macrocycle, H1 and H2 are hydrogen-bonded to O1 and N3, with N1···O1 and N2···N3 distances of 2.766 and 2.715 Å, respectively.

The ^{1}H NMR spectrum of Pd(II) complex **2** in $CDCl_3$ (Fig. S13†) shows nine CH signals in the low field region of δ = 8.93–10.50 ppm, an NH proton in the high field region at δ = −0.93, and a CH proton at δ = −2.85. Compared with free base **1**, **2** exhibits one fewer inner NH, two fewer peripheral CH protons and one more inner CH, indicating that one NH is deprotonated, and one of the heterocycles is inverted with one of its β-CH moieties deprotonated upon coordination with Pd(II). This inference is consistent with the crystal structure (*vide infra*). The ^{1}H NMR spectrum of **3** exhibits eleven peripheral CH protons in the low field region (δ = 8.46–11.28 ppm) and one NH signal at δ = 0.28 ppm (Fig. S15†), indicating that one of the NH moieties in **1** has been deprotonated. Meanwhile, fifteen additional protons are observed with δ = 4.29–6.23 ppm, indicating the coordination of a PPh_3 ligand in the shielding region of the dithiahexaphyrin macrocycle, which is consistent with the crystal structure (*vide infra*). Consistent with the HRMS and NMR data, the crystal structure of **2** unambiguously reveals the coordination of a palladium atom within the cavity composed of rings A, B, C and F. Notably, thiophene ring F is inverted with one of the C–H moieties coordinated in the deprotonated form, and the other C–H remains intact within the macrocycle (Fig. 2c, d and S24†). The coordination bond lengths lie in the range of 1.980–2.086 Å. Within the macrocycle, H2 and H21 are hydrogen-bonded to N3 and O1, with N2···N3 and O1···C21 distances of 2.839 and 2.735 Å, respectively. In contrast to **2**, the crystal structure of **3** reveals the coordination of Pd(II) in another cavity composed of rings C, D, E, and F, with the Pd1 atom coordinated to the N2 and N3 from pyrroles C and D, respectively, in addition to two auxiliary ligands of Cl^- and PPh_3 (Fig. 2e, f and S25†). The distances of Pd1–N2, Pd1–N3, Pd1–P1 and Pd1–Cl lie in the range of 2.010–2.289 Å. Within the macrocycle, H1 is hydrogen-bonded to O1, with the N1···O1 distance of 2.680 Å. Notably, a PPh_3 ligand is located in the shielding facial zone, which is consistent with the ^{1}H NMR data (*vide supra*).

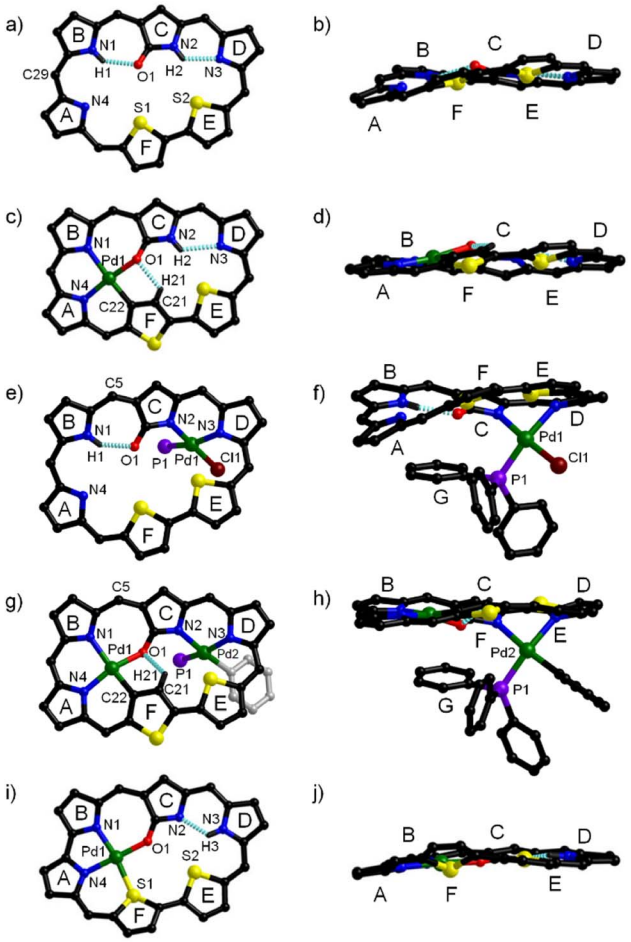

Fig. 2 Complementary views of the molecular structures of **1** (a) and (b), **2** (c) and (d), and **3** (e) and (f), **4-Ph** (g) and (h), and **5** (i) and (j). For clarity, all the C_6F_5 groups, solvents, and the hydrogen atoms attached to the carbon atoms are omitted. In addition, the phenyl groups in the PPh_3 ligands are omitted in figures (e) and (g). The dotted lines represent intramolecular hydrogen bonds.

The ^{1}H NMR spectrum of bis-Pd complex **4-Ph** shows nine CH protons in the low field region (δ = 9.01–10.75 ppm) and one CH proton at δ = −3.78 ppm (Fig. S17†), indicating that further coordination of **2** with the second Pd(II) atom is accompanied with the deprotonation of an NH moiety within the second cavity. Notably, twenty protons appear in the region of δ = 2.27–6.38 ppm, assignable to an ancillary phenyl ligand in addition to a PPh_3 ligand in the shielding zone, which is consistent with the HRMS data (*vide supra*). The ^{1}H NMR spectrum of **4-Cl** shows nine CH in the low field region (δ = 9.10–10.66 ppm) and one CH proton in the high field region (δ = −4.08 ppm) (Fig. S19†), which is similar to that of **4-Ph**, indicating that the dithiahexaphyrin ligand in **4-Cl** coordinates in the mode identical to that in **4-Ph**. However, only fifteen protons appear in the region of δ = 4.22–6.23 ppm, which is consistent with the coordination of a chloro ligand instead of the phenyl ligand in **4-Ph**, as revealed by the HRMS data (*vide supra*). Consistent to the HRMS and NMR data, single crystal X-ray diffraction analysis reveals that **4-Ph** possesses a bis-Pd coordination structure, with two Pd(II) atoms coordinated within the two cavities. Pd1 is coordinated in a NNOC environment donated by rings A, B, C and F, and the inverted thiophene ring F is coordinated in the deprotonated form like that observed in complex **2**. Meanwhile, Pd2 is coordinated to two N atoms donated by pyrrole rings C and D (Fig. 2g, h and S26†). In addition, Pd2 is also coordinated to an ancillary PPh_3 ligand as well as a phenyl ligand, different from that of a chloro ligand in **3**. The coordination bond lengths for Pd1 and Pd2 lie in the ranges of 1.851–2.032 Å and 1.999–2.263 Å, similar to those of **2** and **3**, respectively. Within the cavity, H21 is hydrogen-bonded to O1, with the C21···O1 distance of 2.279 Å. Obviously, the ancillary PPh_3 and Ph^- ligands are located in the shielding facial zone, consistent with

the ^{1}H NMR data (*vide supra*). Although the single crystals of **4-Cl** could not be obtained, **4-Cl** seems to have a bis-Pd(II) coordination structure similar to that of **4-Ph** considering the similar NMR characters (*vide supra*), with a chloro ligand coordinated in place of the Ph^- ligand.

The ^{1}H NMR spectrum of **5** exhibits eleven CH protons in the low field region and one NH proton in the high field region (Fig. S20 and S21†), which is consistent with the mono-Pd(II) coordination structure inferred from the HRMS data (*vide supra*) with one *meso*-carbon and the corresponding C_6F_5 moiety eliminated. Consistently, the crystal structure of **5** reveals that the *meso*-carbon atom between pyrrole rings A and B and the corresponding C_6F_5 moiety have been eliminated, and thus these two pyrrole units are directly linked, and thus a Pd(II) atom is coordinated in an ONNS environment contributed by pyrrole rings A, B, C and thiophene ring F (Fig. 2i, j and S27†). The coordination bond lengths lie in the range of 1.906–2.331 Å. Within the macrocycle, H3 is hydrogen-bonded to N2, with the N2⋯N3 distance of 2.550 Å, which is obviously smaller than the corresponding value in **2** (2.839 Å). Similarly, the respective distances of 3.297 and 4.249 Å for S2⋯N2 and O1⋯N3 are also obviously smaller than the corresponding values of 3.476 and 4.797 Å observed for complex **2**. These data indicate that elimination of the *meso*-carbon atom facilitates the coordination of the sulphur atom, resulting in the shrinking of the remaining noncoordinated cavity, which is unfavourable for further coordination of an additional Pd(II) atom. Consistent to this expectation, we failed to synthesize any bis-Pd complex from **5** irrespective of the palladium reagents used.

It is obvious that the conformation and planarity of the hexaphyrin macrocycles can be effectively modulated by metal coordination. To assess the planarity of the macrocycles, the root mean squared deviation (RMSD) values for all the atoms in the macrocycle can be calculated from the crystal data as a quantitative index.[72,73] As a result, the RMSD value of **1** was calculated to be 0.404 Å, similar that of 0.402 Å obtained for the corresponding all-pyrrole hexaphyrin(1.1.1.1.1.0).[74] Upon coordination of Pd(II) in the cavity composed of A, B, C and F rings, the RMSD value of **2** was calculated to be 0.319 Å, indicating that the coordination results in enhanced planarity. On the other hand, the coordination of Pd(II) in the other cavity results in an obviously larger RMSD value of 0.568 Å for **3**, indicating more severe distortion of the macrocycle compared with that of **1**, which may be related to the good flexibility of the hexaphyrin macrocycle and the steric hindrance associated with the ancillary ligands. However, the bis-Pd(II) coordination in **4-Ph** results in improved planarity with the RMSD value of 0.301 Å, which is smaller than those of **2** (0.319 Å) and **1** (0.404 Å). This observation indicates that the bis-Pd(II) coordination enhances both the rigidity and the planarity of the hexaphyrin macrocycle. Upon *meso*-carbon elimination and coordination of the cavity composed of A, B, C and F rings, **5** exhibits the smallest RMSD value of 0.296 Å among these compounds, indicating the best planarity of the macrocycle.

Based on the crystal structure studies, the absorption spectra of the compounds were measured in CH_2Cl_2 (Fig. 3), which exhibit aromatic features and near-infrared (NIR) absorption. The absorption spectrum of **1** exhibits an intense Soret-like band at 552 nm and two weak Q-like bands at 679 nm and 835 nm, with the band edge of *ca.* 1000 nm. The unsymmetrical mono-Pd(II) complexes **2** and **3** exhibit split Soret-like bands and three weak Q-like bands with the band edges extended to *ca.* 1050 nm. Similarly, mono-Pd(II) complex **5** also shows split Soret-like bands, but the band edge is blue-shifted to *ca.* 980 nm relative to those of **2** and **3**, because of the contracted conjugation structure. On the other hand, the relatively more symmetrical bis-Pd complex **4-Ph** exhibits an intense Soret-like band at 622 nm, and three weak Q-like bands at 760 nm, 870 nm and 984 nm. Compared with **1**, the band-edge of **4-Ph** is about 60 nm red-shifted with the absorption tail extended to *ca.* 1060 nm. Similarly, **4-Cl** exhibits a similar absorption spectrum with an intense Soret-like band at 622 nm, and three weak Q-like bands at 768 nm, 862 nm and 974 nm. Compared with **1**, the band-edge of **4-Cl** is about 40 nm red-shifted with the absorption tail extended to *ca.* 1040 nm. Complexes **2**, **3**, **4-Ph** and **4-Cl** all show red-shifted absorption due to the narrower energy gaps relative to **1**, which may derive from the electronic interaction between the metal atoms and the macrocyclic ligand. Furthermore, the absorption spectra of these compounds simulated by time-dependent density functional theory (TD-DFT) calculations roughly agree with the experimental results (Fig. S28–S33†).

To further probe the aromaticity of the compounds, the anisotropy of the induced current density (ACID) plot, nucleus-independent chemical shift (NICS) and harmonic oscillator model for aromaticity (HOMA) were calculated. Thus, the ACID plots of the compounds all display clockwise ring current along the hexaphyrinoid macrocycle (Fig. S34–S39†), consistent with their 26 π aromatic characters revealed by the ^{1}H NMR data and the crystal structures. The NICS(0) value of −10.3 obtained for **1** is less negative than that of −16.7 obtained for the corresponding all-pyrrole hexaphyrin(1.1.1.1.1.0), indicative of weakened aromaticity of **1**, which can be attributed to the introduction of the weakly aromatic bithiophene unit. The

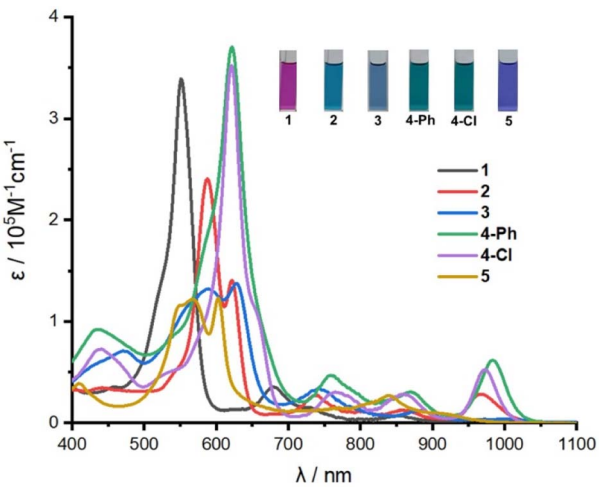

Fig. 3 Absorption spectra of **1**, **2**, **3**, **4-Ph**, **4-Cl**, **5** in CH_2Cl_2. The inset shows the photographs of the corresponding solutions in CH_2Cl_2.

NICS(0) values of palladium complexes **2**, **3**, **4-Ph**, **4-Cl** and **5** were calculated to be −13.4, −13.8, −12.8, −12.2 and −14.2 respectively, more negative than that of **1**, indicating stronger aromaticity of the Pd(II) complexes (Fig. S40†). Consistently, the HOMA values of **2**, **3**, **4-Ph** and **5** were found to be 0.62, 0.77, 0.65 and 0.84, respectively, larger than that of 0.60 calculated for **1** (Fig. S23–S27†). These results indicate that the Pd(II) coordination within the cavities of **1** are favourable for improving the planarity of the macrocycle and thus enhancing the aromatic character. Furthermore, coordination of Pd(II) within the contracted macrocycle afforded the best planarity and strongest aromaticity of **5** among all the complexes.

Notably, different from hexaphyrin(1.1.1.1.1.1) and hexaphyrin(1.1.0.1.1.0),[33–36] dithiahexaphyrin(1.1.1.1.1.0) **1** exhibits a highly unsymmetrical structure due to the incorporation of N-confused pyrrole and bithiophene units, which endows **1** with diverse Pd-complexation behaviour. Different from the 28 π Möbius-aromaticity, nonaromaticity and 24 π Hückel-antiaromaticity observed for the Pd(II) complexes of hexaphyrin(1.1.1.1.1.1) and hexaphyrin(1.1.0.1.1.0), respectively,[33–36] the corresponding Pd(II) complexes of **1** all show 26 π Hückel-aromaticity, which may be related to the relatively good stability of 26 π Hückel-aromaticity for the rigid skeletons incorporating the bithiophene unit. Consistently, the molar extinction coefficients of **1** and its Pd-complexes are noticeably higher than those of hexaphyrin(1.1.1.1.1.1), hexaphyrin(1.1.0.1.1.0) and their Pd-complexes.

Conclusions

In summary, we synthesized 26 π-electron aromatic N-confused dithiahexaphyrin **1** (1.1.1.1.1.0) by incorporating an N-confused pyrrole and a bithiophene into the hexaphyrin framework. Because of the presence of two unsymmetrical cavities, **1** exhibits interesting coordination behaviour, and five palladium complexes have been synthesized under various conditions. Thus, treating **1** with $PdCl_2$ and $(PPh_3)_2PdCl_2$ afforded two mono-Pd(II) complexes **2** and **3**, respectively, with the Pd(II) atom coordinated in the different cavities. On this basis, bis-Pd(II) complexes **4-Ph** and **4-Cl** were synthesized by treating **2** and **3** with $(PPh_3)_2PdCl_2$ and $PdCl_2$, respectively. As a result, both **4-Ph** and **4-Cl** contain two Pd(II) atoms coordinated within the two cavities, with one of the Pd(II) atoms further coordinated to a phosphine ligand as well as an anionic ancillary ligand of Ph^- and Cl^-, respectively. These results indicate that the Pd(II) complexes can be modulated by the reaction sequence of the palladium reagents employed. Notably, treating **1** with $Pd(PPh_3)_4$ afforded a third mono-Pd(II) complex **5**, with the Pd(II) atom coordinated within a further contracted hexaphyrin macrocycle which has been generated from **1** by eliminating one of the *meso*-carbon atoms and the corresponding C_6F_5 moiety. These complexes present 26 π aromaticity and NIR absorption up to 1060 nm, and the absorption can be effectively modulated by Pd(II) coordination, macrocycle contraction and the ancillary ligand coordination. This work may provide an effective approach for synthesizing a series of novel porphyrinoid palladium complexes with tunable structures and properties by employing a single porphyrinoid ligand, which may avoid tedious syntheses of a series of porphyrinoid ligands.

Data availability

Experimental and theoretical details supporting the statements of this article are included in the ESI.†

Author contributions

Conceptualization: Q. Li, Y. Xie; methodology: C. Li, F. Sha, X. Wu, S. Li; synthesis and test: M. Sun; theoretical calculations: G. Baryshnikov, H. Ågren; writing–original draft: M. Sun; writing–review & editing: Y. Xie, Q. Li.

Conflicts of interest

The authors declare no competing financial interest.

Acknowledgements

This work at ECUST was financially supported by NSFC (22131005, 21971063, 22201074, 22075077), the Fundamental Research Funds for the Central Universities, Shanghai Rising-Star Program (23QA1402100), and Natural Science Foundation of Shanghai (23ZR1415600, 22ZR1416100). G. B. thanks for the Swedish National Infrastructure for Computing (SNIC) resources at the High-Performance Computing Center North (HPC2N) and the financial support of the Swedish Research Council (2018-05973, 2020-04600). The authors thank the Research Center of Analysis and Test of East China University of Science and Technology for compound characterization.

Notes and references

1 D. W. Thuita and C. Brückner, *Chem. Rev.*, 2022, **122**, 7990–8052.
2 P. Jiang, T. Zhao, J. Rong, B. Yin, Y. Rao, M. Zhou, L. Xu and J. Song, *Chin. Chem. Lett.*, 2021, **32**, 2562–2566.
3 M. Hou, W. Chen, J. Zhao, D. Dai, M. Yang and C. Yi, *Chin. Chem. Lett.*, 2022, **33**, 4101–4106.
4 J. Zhang, L. Gong, X. Zhang, M. Zhu, C. Su, Q. Ma, D. Qi, Y. Bian, H. Du and J. Jiang, *Chem.–Eur. J.*, 2020, **26**, 13842–13848.
5 I. Yadav, J. K. Sharma, M. Sankar and F. D'Souza, *Chem.–Eur. J.*, 2023, **29**, e202301341.
6 S.-Y. Liu, N. Kishida, J. Kim, N. Fukui, R. Haruki, Y. Niwa, R. Kumai, D. Kim, M. Yoshizawa and H. Shinokubo, *J. Am. Chem. Soc.*, 2023, **145**, 2135–2141.
7 T. Chatterjee, V. S. Shetti, R. Sharma and M. Ravikanth, *Chem. Rev.*, 2017, **117**, 3254–3328.
8 M. Toganoh and H. Furuta, *Chem. Rev.*, 2022, **122**, 8313–8437.
9 R. Misra and T. K. Chandrashekar, *Acc. Chem. Res.*, 2008, **41**, 265–279.
10 H. Maeda, Y. Ishikawa, T. Matsuda, A. Osuka and H. Furuta, *J. Am. Chem. Soc.*, 2003, **125**, 11822–11823.

11 P. J. Chmielewski, L. Latos-Grażyński and T. Glowiak, *Angew. Chem., Int. Ed. Engl.*, 1994, **33**, 779–781.
12 N. Tripathi, A. Sinha and M. Ravikanth, *Org. Biomol. Chem.*, 2023, **21**, 6617–6623.
13 F. D'Souza, *Angew. Chem., Int. Ed.*, 2015, **54**, 4713–4714.
14 T. D. Lash, *Chem. Rev.*, 2017, **117**, 2313–2446.
15 S. Shimizu, *Chem. Rev.*, 2017, **117**, 2730–2784.
16 Y. Matano, *Chem. Rev.*, 2017, **117**, 3138–3191.
17 T. Sarma and P. K. Panda, *Chem. Rev.*, 2017, **117**, 2785–2838.
18 T. Tanaka and A. Osuka, *Chem. Rev.*, 2017, **117**, 2584–2640.
19 B. Szyszko, M. J. Białek, E. Pacholska-Dudziak and L. Latos-Grażyński, *Chem. Rev.*, 2017, **117**, 2839–2909.
20 J. Setsune, *Chem. Rev.*, 2017, **117**, 3044–3101.
21 Q. Li, M. Ishida, C. Li, G. Baryshnikov, F. Sha, B. Zhu, X. Wu, H. Ågren, H. Furuta and Y. Xie, *CCS Chem.*, 2023, **5**, 1332–1342.
22 K. Hurej, M. Pawlicki, L. Szterenberg and L. Latos-Grażyński, *Angew. Chem., Int. Ed.*, 2016, **55**, 1427–1431.
23 A. Ghosh and M. Ravikanth, *Inorg. Chem.*, 2012, **51**, 6700–6709.
24 C.-H. Chuang, C.-K. Ou, S.-T. Liu, A. Kumar, W.-M. Ching, P.-C. Chiang, M. A. C. dela Rosa and C.-H. Hung, *Inorg. Chem.*, 2011, **50**, 11947–11957.
25 C. Brückner, *Acc. Chem. Res.*, 2016, **49**, 1080–1092.
26 Y. Ning, G. Q. Jin and J. L. Zhang, *Acc. Chem. Res.*, 2019, **52**, 2620–2633.
27 Y. Li, M. Zhou, L. Xu, B. Zhou, Y. Rao, H. Nie, T. Gu, J. Zhou, X. Liang, B. Yin, W. Zhu, A. Osuka and J. Song, *Org. Lett.*, 2020, **22**, 6001–6005.
28 Q. C. Chen, M. Soll, A. Mizrahi, I. Saltsman, N. Fridman, M. Saphier and Z. Gross, *Angew. Chem., Int. Ed.*, 2018, **57**, 1006–1010.
29 M. G. P. M. S. Neves, R. M. Martins, A. C. Tomé, A. J. D. Silvestre, A. M. S. Silva, V. Félix, J. A. S. Cavaleiro and M. G. B. Drew, *Chem. Commun.*, 1999, 385–386.
30 T. Sarma, G. Kim, S. Sen, W.-Y. Cha, Z. Duan, M. D. Moore, V. M. Lynch, Z. Zhang, D. Kim and J. L. Sessler, *J. Am. Chem. Soc.*, 2018, **140**, 12111–12119.
31 S. Mori and A. Osuka, *J. Am. Chem. Soc.*, 2005, **127**, 8030–8031.
32 T. Nédellec, B. Boitrel and S. Le Gac, *J. Am. Chem. Soc.*, 2023, **145**, 27067–27079.
33 S. Mori, S. Shimizu, R. Taniguchi and A. Osuka, *Inorg. Chem.*, 2005, **44**, 4127–4129.
34 T. Tanaka, T. Sugita, S. Tokuji, S. Saito and A. Osuka, *Angew. Chem., Int. Ed.*, 2010, **49**, 6619–6621.
35 M. Inoue and A. Osuka, *Angew. Chem., Int. Ed.*, 2010, **49**, 9488–9491.
36 F. Luo, L. Liu, H. Wu, L. Xu, Y. Rao, M. Zhou, A. Osuka and J. Song, *Nat. Commun.*, 2023, **14**, 5028.
37 S. Mori and A. Osuka, *Inorg. Chem.*, 2008, **47**, 3937–3939.
38 K. Shimomura, H. Kai, Y. Nakamura, Y. Hong, S. Mori, K. Miki, K. Ohe, Y. Notsuka, Y. Yamaoka, M. Ishida, D. Kim and H. Furuta, *J. Am. Chem. Soc.*, 2020, **142**, 4429–4437.
39 A. Srinivasan, T. Ishizuka, A. Osuka and H. Furuta, *J. Am. Chem. Soc.*, 2003, **125**, 878–879.
40 K. Yamasumi, K. Nishimura, Y. Hisamune, Y. Nagae, T. Uchiyama, K. Kamitani, T. Hirai, M. Nishibori, S. Mori, S. Karasawa, T. Kato, K. Furukawa, M. Ishida and H. Furuta, *Chem.–Eur. J.*, 2017, **23**, 15322–15326.
41 T. K. Chandrashekar and S. Venkatraman, *Acc. Chem. Res.*, 2003, **36**, 676–691.
42 A. Alka, V. S. Shetti and M. Ravikanth, *Coord. Chem. Rev.*, 2019, **401**, 213063.
43 S. Gokulnath, K. Yamaguchi, M. Toganoh, S. Mori, H. Uno and H. Furuta, *Angew. Chem., Int. Ed.*, 2011, **50**, 2302–2306.
44 Y. Wang, H. Kai, M. Ishida, S. Gokulnath, S. Mori, T. Murayama, A. Muranaka, M. Uchiyama, Y. Yasutake, S. Fukatsu, Y. Notsuka, Y. Yamaoka, M. Hanafusa, M. Yoshizawa, G. Kim, D. Kim and H. Furuta, *J. Am. Chem. Soc.*, 2020, **142**, 6807–6813.
45 H. Shu, M. Guo, M. Wang, M. Zhou, B. Zhou, L. Xu, Y. Rao, B. Yin, A. Osuka and J. Song, *Angew. Chem., Int. Ed.*, 2022, **61**, e202209594.
46 Y. Liu, D. Xie, Y. Rao, L. Xu, M. Zhou, A. Osuka and J. Song, *Angew. Chem., Int. Ed.*, 2022, **61**, e202206601.
47 L. Liu, Z. Hu, F. Zhang, Y. Liu, L. Xu, M. Zhou, T. Tanaka, A. Osuka and J. Song, *Nat. Commun.*, 2020, **11**, 6206.
48 Y. Rao, L. Xu, M. Zhou, B. Yin, A. Osuka and J. Song, *Angew. Chem., Int. Ed.*, 2022, **61**, e202206899.
49 Y. Xu, B. Zhu, Q. Li, F. Sha, G. Baryshnikov, L. He, Y. Feng, J. Tang, Y. Wei, C. Li, X. Wu, H. Ågren and Y. Xie, *Org. Lett.*, 2023, **25**, 1793–1798.
50 T. Yoneda and A. Osuka, *Chem.–Eur. J.*, 2013, **19**, 7314–7318.
51 S. Gokulnath, K. Nishimura, M. Toganoh, S. Mori and H. Furuta, *Angew. Chem., Int. Ed.*, 2013, **52**, 6940–6943.
52 Q. Li, M. Ishida, H. Kai, T. Gu, C. Li, X. Li, G. Baryshnikov, X. Liang, W. Zhu, H. Ågren, H. Furuta and Y. Xie, *Angew. Chem., Int. Ed.*, 2019, **58**, 5925–5929.
53 Y. Du, B. Zhu, Q. Li, G. Baryshnikov, C. Wei, Y. Lin, G. Su, C. Li, H. Ågren and Y. Xie, *Org. Lett.*, 2020, **22**, 9648–9652.
54 G. Su, Q. Li, M. Ishida, C. Li, F. Sha, X.-Y. Wu, L. Wang, G. Baryshnikov, D. Li, H. Ågren, H. Furuta and Y. Xie, *Angew. Chem., Int. Ed.*, 2020, **59**, 1537–1541.
55 Q. Li, M. Ishida, Y. Wang, C. Li, G. Baryshnikov, B. Zhu, F. Sha, X. Wu, H. Ågren, H. Furuta and Y. Xie, *Angew. Chem., Int. Ed.*, 2023, **62**, e202212174.
56 W. Y. Gao, M. Chrzanowski and S. Ma, *Chem. Soc. Rev.*, 2014, **43**, 5841–5866.
57 J. W. Buchler, *J. Porphyrins Phthalocyanines*, 2000, **04**, 337–339.
58 T. D. Lash, *Chem.–Asian J.*, 2014, **9**, 682–705.
59 C. Wu, X. Li, M. Shao, J. Kan, G. Wang, Y. Geng and Y.-B. Dong, *Chin. Chem. Lett.*, 2022, **33**, 4559–4562.
60 Z. Liang, H. Guo, H. Lei and R. Cao, *Chin. Chem. Lett.*, 2022, **33**, 3999–4002.
61 B. Babu, J. Mack and T. Nyokong, *Dalton Trans.*, 2023, **52**, 5000–5018.
62 C. Liu, K. Liu, C. Wang, H. Liu, H. Wang, H. Su, X. Li, B. Chen and J. Jiang, *Nat. Commun.*, 2020, **11**, 1047.
63 T. Sakurai, Y. Hiraoka, H. Tanaka, Y. Miyake, N. Fukui and H. Shinokubo, *Angew. Chem., Int. Ed.*, 2023, **62**, e202300437.

64 G. I. Vargas-Zúñiga and J. L. Sessler, *Coord. Chem. Rev.*, 2017, **345**, 281–296.
65 J. Luo, Z. Xie, J. Zou, X. Wu, X. Gong, C. Li and Y. Xie, *Chin. Chem. Lett.*, 2022, **33**, 4313–4316.
66 J. Zou, Y. Wang, G. Baryshnikov, J. Luo, X. Wang, H. Ågren, C. Li and Y. Xie, *ACS Appl. Mater. Interfaces*, 2022, **14**, 33274–33284.
67 C. Li, K. Zhang, M. Ishida, Q. Li, K. Shimomura, G. Baryshnikov, X. Li, M. Savage, X.-Y. Wu, S. Yang, H. Furuta and Y. Xie, *Chem. Sci.*, 2020, **11**, 2790–2795.
68 A. Nakai, T. Yoneda, T. Tanaka and A. Osuka, *Chem. Commun.*, 2021, **57**, 3034–3037.
69 D. Comandella, M. Werheid, F.-D. Kopinke and K. Mackenzie, *Chem. Eng. J.*, 2017, **319**, 21–30.
70 J. Zhu, J. Wood, K. Deplanche, I. Mikheenko and L. E. Macaskie, *Appl. Catal., B*, 2016, **199**, 108–122.
71 J. Y. Shin, H. Furuta, K. Yoza, S. Igarashi and A. Osuka, *J. Am. Chem. Soc.*, 2001, **123**, 7190–7191.
72 H. Matsumoto, T. Okujima, S. Mori, A. C. C. Bacilla, M. Takase, H. Uno and N. Kobayashi, *Org. Lett.*, 2021, **23**, 3442–3446.
73 Y. Xu, B. Zhu, Q. Li, G. Baryshnikov, M. Zhou, C. Li, F. Sha, X. Wu, H. Ågren, J. Song and Y. Xie, *Org. Lett.*, 2021, **23**, 8307–8311.
74 X.-J. Zhu, S.-T. Fu, W.-K. Wong, J.-P. Guo and W.-Y. Wong, *Angew. Chem., Int. Ed.*, 2006, **45**, 3150–3154.